Journal of Applied Electrochemistry (2006) 36:187–193
DOI 10.1007/s10800-005-9051-5

On efficiency of both single fuel cells and stacks II

ROBERTO C. DANTE[1,*], FRANK MENZL[2], JOCHEN LEHMANN[2], CHRISTIAN SPONHOLZ[2], ORTRUD LUSCHTINETZ[2] and OMAR SOLORZA-FERIA[3]
[1]*Renewable Energy Center, Basic Sciences Department, Engineering Division, Instituto Tecnológico de Monterrey, in Mexico City, Calle del Puente 222, Col. Ejidos de Huipulco, 14380, Mexico City, Mexico*
[2]*Electrical Techniques Faculty, Fachhochschule Stralsund (University of Applied Sciences), Zur Schwedenschanze 15, 18435, Stralsund, Germany*
[3]*Chemistry Department, Centro de Investigaciones y Estudios Avanzados (CINVESTAV), Instituto Politécnico Nacional, Av. Instituto Politécnico Nacional 2508 Col. San Pedro Zacatenco, 07360, Mexico City, Mexico*
*(*author for correspondence, fax: +0052-55-54832163; e-mail: rdante@itesm.mx)*

Received 16 February 2005; accepted in revised form 16 August 2005

Key words: fuel cell efficiency, fuel cell thermodynamics, polarization curve, stack reaction extent, stack utilization

Abstract

The model developed in the first part of this work is used to predict the cell potentials and the irreversible Gibbs free energy of a stack of 15 cells. The model starts from a phenomenological equation of a polarization curve with the extent of reaction as the independent variable. Two extreme kinds of flow of reagents, defined as Chain and Separate Flows respectively, are considered. The cell potentials are obtained by a combination of the potential of the two extreme cases of flow. The stack cell potentials and the efficiencies, estimated by the model, reproduce the general characteristics obtained by the experiments.

1. Introduction

The efficiency of stacks made of identical cells can be predicted by means of thermodynamic tools and a model of cell potential variation along the stack, with the extent of reaction as an independent variable. The irreversible processes occurring in a fuel cell stack have the potential to decline along the stack. The average potential of the stack is used to determine the stack efficiency [1–7], as the following equation shows

$$\eta = \frac{c\bar{U}F\xi_s}{\Delta H} = \frac{\Delta G}{\Delta H}; \tag{1}$$

where c corresponds to the number of electrons exchanged by the reaction, $\bar{U}$ is the average potential, F is the Faraday constant, ξ_s is the stack extent of reaction, ΔH and ΔG are the enthalpy and the Gibbs free energy, respectively [8].

In this paper, experimental cell potentials are reported for a stack of 15 cells. These results are compared with model predictions. The efficiency calculated by means of the experimental average potential of the stack is also compared with the efficiency calculated through the model. The flow of reagents along the stack was previously classified in two cases: Chain Flow and Separate Flow. In Figure 1, the two cases are schematically shown. In the Chain Flow stack the same stream of reagents passes consecutively through each cell, while in the Separate Flow a main stream is divided in many equal flows as cells. Real fuel cell stacks have hybrid flow connections and manifest a behavior that reflects a combination of these two cases. During operation, stacks with Separate feeding also have a gradient of flow rates along the stack, as do the Chain stacks [9]. The considered stack is a Separate Flow fuel cell stack of the type indicated in Figure 2. A marked transition of behavior from a Separate Flow type to a full Chain type was predicted at high utilization, by means of thermodynamics [9].

2. Model and methodology

The basis of the proposed model, described in detail in a previous paper [9], is the polarization curve equation [10–13] given here:

$$U_q(\xi_q, p_{qj}, T) = \alpha_1 - \alpha_2\xi_q - \alpha_3 \ln \xi_q - \alpha_4 \exp \alpha_5\xi_q + \alpha_6 \ln \prod_j (p_{qj}/p_{1j})^{\nu_j} \tag{2}$$

The six α_i parameters are determined by fitting an experimental polarization curve, with the exception of

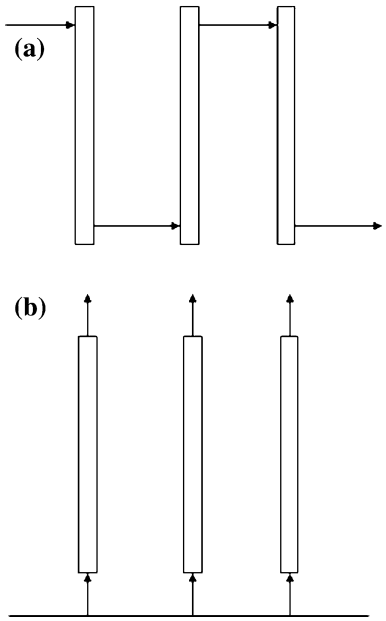

Fig. 1. (a) Chain Flow, (b) Separate Flow.

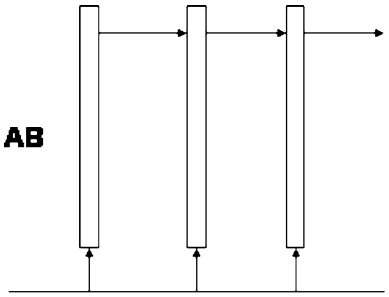

Fig. 2. Intermediate case between the extreme cases of flows (a) and (b).

α_6, to which the value of 0.013 is assigned, and corresponds to the ratio RT/nF of Nernst equation. In Equation 2, p_{qj} is the partial pressure of reagent j in the cell q, p_{1j} is the partial pressure of reagent j in the first cell, and ξ_q is the extent of reaction of the cell q, as defined in the Chain Flow case:

$$\xi_q = \frac{\xi_1}{1-(q-1)\xi_1}, \tag{3.1}$$

$$\xi_s = n\xi_1. \tag{3.2}$$

In Equation 3.1, ξ_1 is the extent of reaction of the first cell, ξ_s is the stack extent of reaction and n the total number of stack cells. The partial pressures are determined in the following way for the reagent in direct flow:

$$p_{qj} = p_{1j}[1-(q-1)u_{1j}] \tag{4}$$

The partial pressures are determined in this way for the reagent in counter flow:

$$p_{qj} = p_{nj}[1-(n-q)u_{nj}] \tag{5}$$

In the Separate Flow case, the extent of reaction and pressure are the same for each cell:

$$\xi_q = \xi = \xi_s, \tag{6}$$

$$p_{qj} = p_j \tag{7}$$

The irreversible Gibbs free energy is experimentally determined in the following way:

$$\Delta G = cF\bar{U}\xi_s; \tag{8.1}$$

where the average stack potential $\bar{U}$ is so defined:

$$\bar{U} = \frac{1}{n}\sum\nolimits_q U_q. \tag{8.2}$$

In order to verify that the model predictions are in agreement with experimental results, the experimental Gibbs free energy obtained by Equations 8.1 and 8.2 is compared with model results obtained in the previous paper [9].

The model determination of ΔG is obtained by means of a linear combination of Gibbs free energy of the pure Separate Flow (Se), and of the Gibbs free energy of the pure Chain Flow (Ch):

$$\begin{aligned}\Delta G &= (1-k)(cF\bar{U}_{\mathrm{Ch}}\xi_s)_{\mathrm{Ch}} + k(cFU_{\mathrm{Se}}\xi)_{\mathrm{Se}} \\ &= (1-k)\Delta G_{\mathrm{Ch}} + k\Delta G_{\mathrm{Se}}, \quad 1 \le k \le 0;\end{aligned} \tag{9.1}$$

$$\bar{U} = (1-k)\bar{U}_{\mathrm{Ch}} + kU_{\mathrm{Se}}, \quad 1 \le k \le 0; \tag{9.2}$$

$$U_q = (1-k)U_{q\mathrm{Ch}} + kU_{\mathrm{Se}}, \quad 1 \le k \le 0. \tag{9.3}$$

It is noteworthy to remember that, for the Separate Flow, the extent of reaction of each cell is the same, thus the average potential U_{Se} coincides with the cell potential and that ξ_s and ξ are the same in Equation 9.1. The coefficient k, at different extents of reaction, is determined by fitting of experimental data. In the discussion of this paper (Section 5), a method to estimate the coefficients k is suggested, leaving aside the fitting of experimental data.

3. Experimental part

A stack composed of 15 cells is considered; each Protonic Exchange Membrane (PEM) cell was manufactured by SZW (Zentrum für Sonnenenergie-und-Wasserstoff-Forschung), with an active area A of 100 cm^2. The stack has a water cooling system which permits to control the temperature. The single cell used to obtain the basic polarization curve is also a SZW, identical to those forming the stack and tested by means of the FCATS screener test station by Hydrogenics Co., at the University of Applied Sciences, Stralsund, Germany [9].

The test conditions for the single cell were: cell temperature 298 K, air flow rate 600 ml min^{-1}

(9.37×10^{-5} mol-O_2 s^{-1}), hydrogen flow rate 150 ml min^{-1} (1.12×10^{-4} mol-H_2 s^{-1}). Where the limiting reagent was hydrogen, the pressure of both gases was 100 kPa, and the humidity was 35%. The equation used to describe its polarization curve is:

$$U(\xi, 100\,kPa, 298\,K) = 0.826 - 0.378\xi - 0.0176\ln\xi - 1.0077\times10^{-5}\exp(10.74\xi); \quad (10)$$

In Figure 3, the polarization curve (solid line) obtained from Equation 10 is shown.

The test conditions of the stack of 15 cells were: hydrogen flow rate 6.27×10^{-4} mol-H_2 s^{-1}, and oxygen flow rate of 6.82×10^{-3} mol-O_2 s^{-1}. The pressure of both gases was 10 kPa. The temperature of the stack cells was about 298–300 K during the tests. In the middle cells the external temperature was about 1 K higher than in the extreme cells. The temperature used for the model calculation was 298 K. Equation 11 allows us to estimate the polarization curve of a single cell at these initial pressures of reagents (oxygen is in counter flow), and provides the proper α_1 term for our basic equation of polarization curve (Equation 2):

$$\begin{aligned} U(\xi, p_{H_2}, p_{O_2}, 298\,K) &= 0.826 - 0.378\xi - 0.0176\ln\xi \\ &- 1.0077\times10^{-5}\exp(10.74\xi) + 0.013\ln\left(\frac{p_{1H_2}p_{nO_2}^{0.5}}{100\times100^{0.5}}\right) \\ &= 0.751 - 0.378\xi - 0.0176\ln\xi - 1.0077 \\ &\times10^{-5}\exp(10.74\xi) \end{aligned} \quad (11)$$

In Figure 3, the polarization curve of the single cell, at these the test conditions and calculated by Equation 11, is shown by a dotted line. Its potential values are lower than those at 100 kPa.

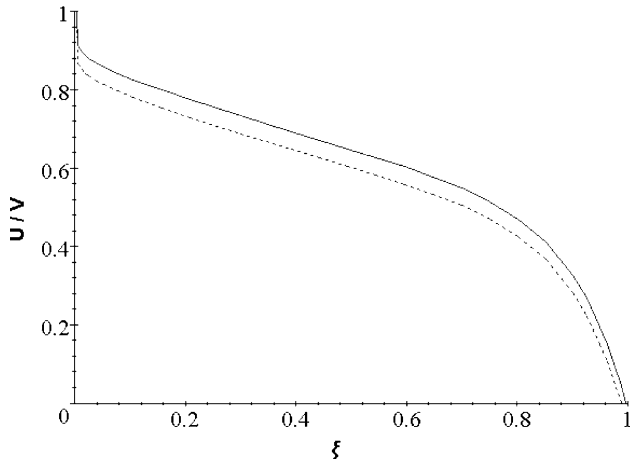

Fig. 3. Polarization curves at 100 kPa, pressure of both gases, (solid line) and at 10 kPa, pressure of both gases (dotted line).

4. Results

The cell potentials of a stack of 15 cells are reported in Figure 4 at different extents of reaction. The average cell potential is 0.862 V, at the stack extent of reaction 0.038, and the average potential falls to 0.62 V, at the stack extent of reaction ξ_s of 0.9. However, the cell potential decays also with increasing the cell number q. At the extent of reaction of 0.9, the potential is of about 0.65 V in the first cell and 0.55 V in the last cell, because of the increment of the cell extent of reaction along the stack [9]. This potential decay is more pronounced when the stack extent of reaction is higher. The model results, obtained using Equations 2–5, are shown in Figure 5. There is substantial agreement between model and experiments. The discrepancy can be due to the fact that, in a real stack, not all the cells are truly identical (small changes can occur due to preparation or interconnection). Another significant discrepancy occurs at high extent of reaction, where the model overestimates the potential decay. The source of this overestimation can be the temperature variation; because, although temperature was controlled, small increments of the

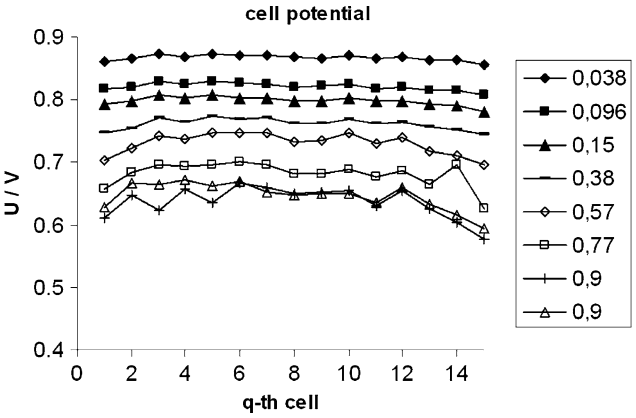

Fig. 4. Experimental cell potentials of a stack of 15 cells. On the right side, the stack extents of reaction are indicated.

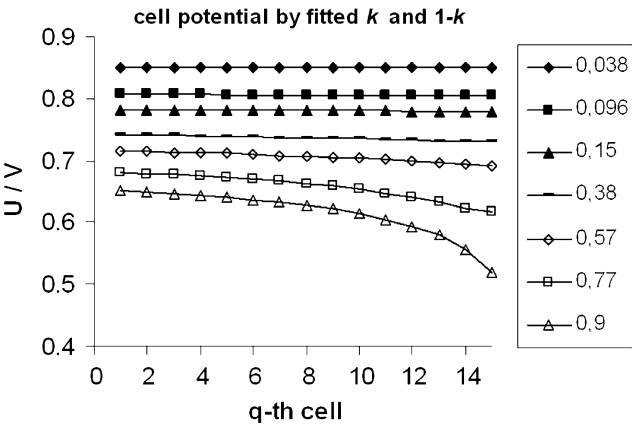

Fig. 5. Cell potentials in a stack of 15 cells, obtained by the fitted k and $1-k$ coefficients. On the right side, the stack extents of reaction are indicated.

internal temperature of the cells can cause an increase of the potential.

The fitted coefficients k and $1-k$ of Equations 9.1–9.3, which are used for the calculation of the model cell potential, are reported in Figure 6. The coefficient k exhibits a maximum at approximately the extent of reaction of 0.2. After the maximum, k decreases slowly until the extent of reaction is 0.8, and then the decay is dramatic.

The experimental Gibbs free energies of the fuel cell stack at different extents of reactions are compared to the Gibbs free energies, obtained from the model and the fitted coefficients k, in Figure 7. The calculations were carried out directly, by means of Equation 8.1 for experimental results, and Equations 8.1–9.3 for the model case. A slight discrepancy between model and experimental values begins at $\xi_s = 0.57$.

5. Discussion

The coefficients k were determined by the fitting of the experimental cell potentials; however, an alternative method could be represented by the framework of the thermodynamics of irreversible processes [14], from which the following expression can be written:

$$\begin{aligned}\Delta G &= -T\Delta S = -T(L_{11}A_1^2 + 2L_{12}A_1A_2 + L_{22}A_2^2) \\ &= L_{\mathrm{ChCh}}\Delta G_{\mathrm{Ch}}^2 + 2L_{\mathrm{ChSe}}\Delta G_{\mathrm{Ch}}\Delta G_{\mathrm{Se}} + L_{\mathrm{SeSe}}\Delta G_{\mathrm{Se}}^2\end{aligned}, \tag{12}$$

if the term $V{\cdot}\Delta p$ of the Gibbs free energy is neglected; where V is the total volume passed through the cell membranes and Δp the total pressure difference within the stack cells. In Equation 12, A is the affinity function, the subscripts 1 and 2 indicate two driving pathways. It is noteworthy that, in Equation 12, it is assumed that the coefficient L_{12} is equal to L_{21}, which is not generally assured in situations far from the equilibrium.

Moreover, in these situations, the coefficients L of Equation 12 could depend on the thermodynamic forces. The following functions were assigned to the coefficients L:

$$L_{\mathrm{ChCh}} = \frac{1}{\Delta G_{\mathrm{Ch}}}; \tag{13.1}$$

$$L_{\mathrm{ChSe}} = -\frac{1}{4\Delta G_{\mathrm{Ch}}}; \tag{13.2}$$

$$L_{\mathrm{SeSe}} = \frac{1}{2\Delta G_{\mathrm{Ch}}}; \tag{13.3}$$

These equations satisfy the requirements that ΔG tends to ΔG_{Ch}, when ξ_s tends to 1 and $\Delta G_{\mathrm{Se}} \to 0$, simultaneously:

$$\lim_{\xi_s \to 1} \Delta G = \lim_{\xi_s \to 1} \left(\Delta G_{\mathrm{Ch}} - \frac{1}{2}\Delta G_{\mathrm{Se}} + \frac{1}{2\Delta G_{\mathrm{Ch}}}\Delta G_{\mathrm{Se}}^2 \right) = \Delta G_{\mathrm{Ch}}; \tag{14.1}$$

and that, at ξ_s tending to 0, when the Gibbs free energies of Chain and Separate cases tend to coincide $\Delta G_{\mathrm{Ch}} \approx \Delta G_{\mathrm{Se}}$, Equation 12 should be reduced to the following arithmetic average:

$$\begin{aligned}\lim_{\xi_s \to 0} \Delta G &= \lim_{\xi_s \to 0} \left(\Delta G_{\mathrm{Ch}} - \frac{1}{2}\Delta G_{\mathrm{Ch}} + \frac{1}{2}\Delta G_{\mathrm{Se}} \right) \\ &= \frac{1}{2}(\Delta G_{\mathrm{Ch}} + \Delta G_{\mathrm{Se}}).\end{aligned} \tag{14.2}$$

The factor 1/2 of Equations 14.1 and 14.2 corresponds to the linear coefficients in situations next to equilibrium.

On the other hand, the coefficients k and $1-k$ become:

$$k = \frac{\Delta G_{\mathrm{Se}}}{2\Delta G_{\mathrm{Ch}}}; \tag{15.1}$$

$$1 - k = \frac{2\Delta G_{\mathrm{Ch}} - \Delta G_{\mathrm{Se}}}{2\Delta G_{\mathrm{Ch}}}; \tag{15.2}$$

calculated by this method, the coefficients k and $1-k$ are shown in Figure 8. The general trends of these coefficients are similar to the experimentally fitted values

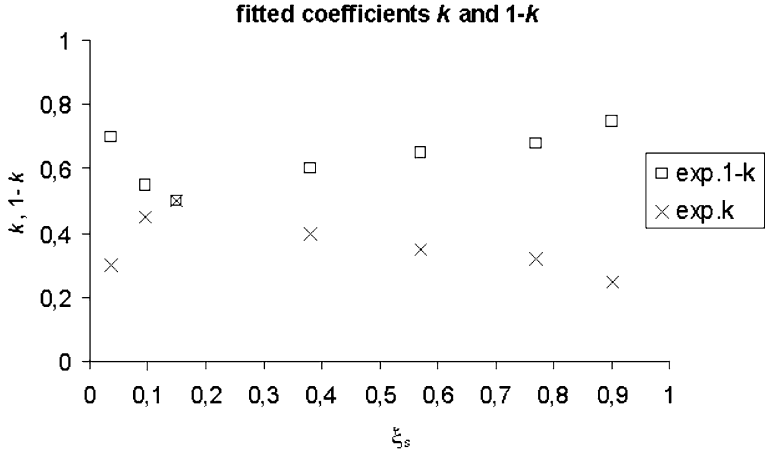

Fig. 6. Coefficients k and $1-k$ used to fit the experimental cell potentials of the stack of 15 cells.

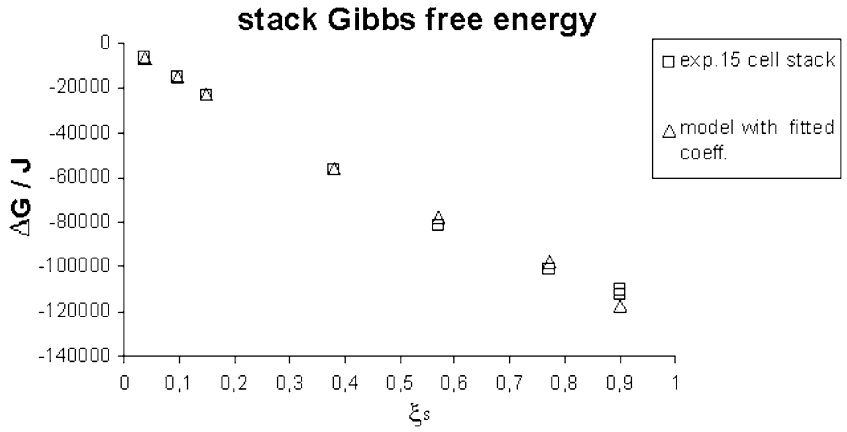

Fig. 7. Comparison of experimental stack Gibbs free energy and the Gibbs free energy obtained applying the model and the fitted coefficients k and $1-k$.

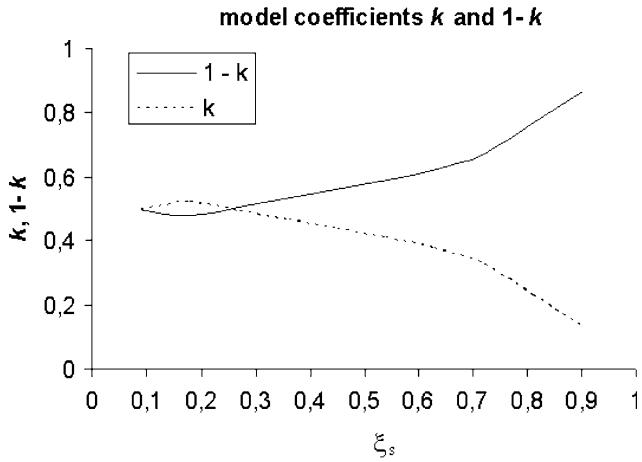

Fig. 8. Coefficients k and $1-k$ calculated through coefficients L of Equations 13.1–13.3.

(Figure 6), but there is an overall discrepancy, at low extents of reaction.

In Figure 9, the Gibbs free energies obtained by means of the coefficients L of Equations 13.1–13.3 are first compared to Chain and Separate Flows Gibbs free energies (calculated in the previous paper [9]). Then they are compared with the experimental Gibbs free energies (calculated by Equation 8.1), and, finally, with the average of Gibbs free energies of the Chain and Separate Flows (the limit case of Equation 14.2). As predicted by Equation 14.2, at low extent of reaction, the Gibbs free energy of the stack coincides with the average Gibbs free energies of the Chain and Separate cases; on the other hand, at higher extent of reaction, after a slight deviation, the values tend to approach the Gibbs free energy of the Chain flow case (Equation 14.1). The intermediate thermodynamic behavior corresponds to an intermediate case of flow, between the two extremes of Chain and Separate Flows (see Figure 2). There is a significant discrepancy between model predictions of Gibbs free energy using Equations 12–13.3 (Figure 7) and experimental Gibbs free energies, at high extent of reaction. This could be ascribed to the term $V{\cdot}\Delta p$ which is neglected in Equation 12 and acquires more importance upon increasing the extent of reaction.

In Figure 10, the efficiencies of the stack calculated by Equation 1 and experimental data are compared to those obtained by model and coefficients L (Equations 13.1–13.3).

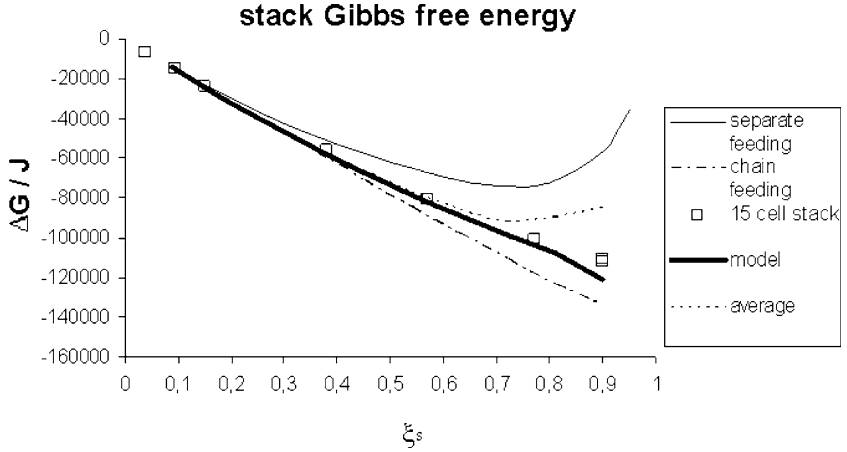

Fig. 9. Stack Gibbs free energy: upper curve, Separate Flow; dotted line, average between Separate Flow and Chain Flow; boxes, experimental results; solid bold line, model with proposed coefficients L; and lower curve Chain Flow.

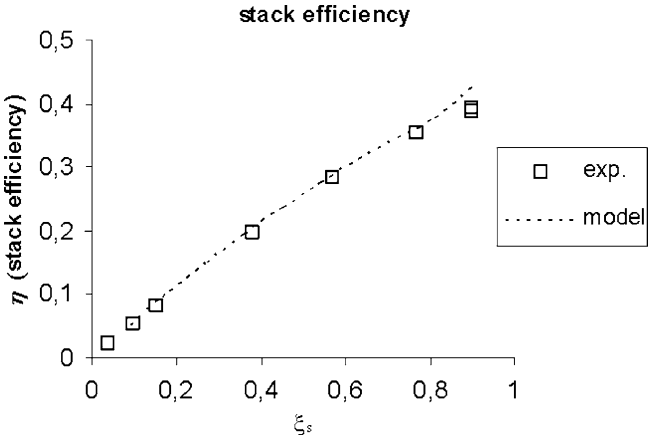

Fig. 10. Efficiency calculated by model and coefficients L (dotted line) and the efficiency calculated by the experimental results (boxes).

The efficiency increases with the stack extent of reaction increment, reaching up to 0.39 at the stack extent of reaction of 0.9. The efficiency, calculated by model coefficients L, is overestimated at higher extents of reaction, e.g. the model predicts the efficiency of 0.42 at the stack extent of reaction of 0.9; however, at lower stack extent of reaction, the agreement is good.

6. Conclusions

The model developed in the first paper of this work [9] is used to predict potential and irreversible Gibbs free energy in a stack of 15 cells. The model starts from a phenomenological model of a polarization curve with the extent of reaction as an independent variable (Equations 2–7, 10 and 11). Two extreme kinds of flows, Chain and Separate Flow, are considered (Figure 1); however, a real fuel cell stack manifests a hybrid of these two cases (Figure 2). The stack cell potentials are obtained by a combination of the potential of the two extreme cases (Chain and Separate Flows). The parameters k and $1-k$ of this combination (Equations 9.1–9.3) are obtained by the fitting of experimental results (Figure 6). The stack cell potentials, obtained from this model (Figure 5), reproduce the general characteristics obtained by experiment (Figure 4). Nevertheless, at high stack extents of reaction the potential decay of the last cells is overestimated by this model (Figure 5). This overestimation can be due to small internal temperature variations of the cells. In this model the temperature was taken constant at 298 K. The model would be improved with the introduction of the temperature as a variable. Nevertheless, the model works in a satisfactory manner for the determination of both the efficiency and the Gibbs free energies, which was the main objective of this paper. The irreversible stack Gibbs free energies and efficiencies obtained from experiments are compared to those obtained by the fitted parameters k and by the coefficients L (Figures 7, 9, 10). The latter were estimated by a combination of the Gibbs free energies of the two extreme cases (Figure 8), taking into account the limit cases of the stack extent of reaction $\xi_s \to 0$ and $\xi_s \to 1$ (Equations 14.1–14.2), and by means of the framework of irreversible thermodynamics (Equations 12–13.3). This achievement opens the possibility to predict the stack efficiency (Figure 10), starting from the model of a polarization curve.

Acknowledgments

The Deutscher Akademischer Austausch Dienst (German Academic Exchange Service), DAAD, supported the stay of Prof. R. Dante at the Fachhochschule Stralsund.

References

1. A.E. Lutz, R.S. Larson and J. Keller, *Int. J. Hydrogen Energy* **27** (2002) 1103.
2. A. Kazim, *Energ. Convers. Manage.* **45** (2004) 1949.
3. Y.A. Cengel and M.A. Boles, 'Thermodynamics – An Engineering Approach'', 2nd ed. (Mc Graw-Hill, Inc., 1994).
4. P.F. Oosterkamp, A.A. Goorse and L.J. Blomen, *J. Power Sources* **41** (1993) 239.
5. K. Kordesch and G. Simader, 'Fuel Cells and Their Applications', (VCH, 1996).
6. E. Chen, *in* Gregor Hoogers (Ed), 'Thermodynamics and Electrochemical Kinetics', Fuel Cell Technology Handbook (CRC Press LLC, 2003) Ch. 3, pp. 3.1–3.30.
7. A. Weber, R. Darling, J. Meyers and J. Newman, ' Mass Transfer at Two-Phase and Three-Phase Interfaces', Fundamentals and Survey of Systems, Handbook of Fuel Cells, Fundamental Technology and Applications, Vol. 1, Ch. 7 (Ed. Wiley, 2003), pp. 47–69.
8. A.K. Demin, P.E. Tsiakaras, V.A. Sobyanin and S.Yu. Hramova, *Solid State Ionics* **152–153** (2002) 55.
9. R.C. Dante, J. Lehmann and O. Solorza-Feria, *J. Appl. Electrochem.* **35**(3) (2005) 327.
10. J. Bockris and S. Srinivasan, *"Fuel Cells: Their Electrochemistry"* (Mc Graw Hill, New York, 1969).
11. J. Kim, S.M. Lee, S. Srinivasan and C.E. Chamberlin, *J. Electrochem. Soc.* **142** (1995) 2670.

12. T.E. Springer, T.A. Rockward, T.A. Zawodzinski and S. Gottesfeld, *J. Electrochem. Soc.* **148**(1) (2001) A11.
13. J. Newman, *Electrochim. Acta* **24** (1979) 223.
14. D.A. McQuarrie and J.D. Simon, *"Molecular Thermodynamics"* (University Science Books, Sauzalito, California, USA, 1999), pp. 581–638.